Biological insights and technical obstacles during rapid at-line single-cell analysis of algal cultures based on label-free flow cytometry

Michael Sandmann (sandmann@hs-nb.de)
University of Applied Sciences Neubrandenburg
Michael Rading
Max Planck Institute of Colloids and Interfaces

Article

Keywords:

Posted Date: May 25th, 2022

DOI: https://doi.org/10.21203/rs.3.rs-1670334/v1

Abstract

The potential of label-free flow cytometry (FC) for bioprocess monitoring was determined for its application to model cultures of *Chlamydomonas.* A theoretical approach based on Lorenz-Mie theory revealed that the storage compounds within algal cells, specifically lipid bodies and starch granules, are the most important contributors to the commonly used wideangle light scattering signal in FC devices. As a result of cellular growth dynamics, a pronounced nonlinearity appeared in the FC data which resulted in distorted chlorophyll and wide-angle scatter distributions. In relation to the nonlinearity, the potential of label-free FC as a tool to follow trajectories of cellular development was determined and revealed high cellto-cell heterogeneity for cellular chlorophyll amount and the wide-angle light scattering signal, showing a spread of about one order of magnitude. Over the developmental cycle, a linear correlation was observed between mean values of the distributions of cellular chlorophyll amount and the wide-angle light scattering signal. Surprisingly, on the singlecell level a relatively low but dynamic correlation over time was observed. Additionally, the mother cells within the cell population differentiated into two subpopulations. In conclusion, nonparallel development of the algal cells was revealed, which expands the view about synchronicity in algal cultures.

Introduction

Modern biology approaches are often based on large collections of quantitative empirical data such as lipid, metabolite, transcript, and protein levels[1,2]. These omics technologies have been some of the key drivers of scientific progress in biology and medicine but are limited to delivering mean values across all cells analyzed in the sample. This means any conclusions drawn from this analysis depend on assuming a homogenous cell population. Single-cell analysis (SCA) can overcome these problems and reveal heterogeneity in cell populations or dynamics within subpopulations[3,4,5,6]. In recent years it has been revealed that complex single-cell dynamics seem to be a major reason behind limitations in productivity of cell cultures in biotechnological production processes[4,6,7]. In these cases, subpopulations of cells emerge that do not take part in the intended production process, ultimately leading to a decrease in profit.

Probably the most common technique for SCA is flow cytometry (FC). It is based on the interaction of single cells with a laser beam and quantification of the optical effects that result from this interaction. Briefly, the cells are suspended in a carrier liquid and pass through a laser beam inside a flow cuvette. Typically, light scattering intensity is analyzed at two different scattering angles and fluorescent properties, arising either from intrinsic pigments or externally applied fluorescent probes[8,9,10]. The wideangle light scattering intensity, also known as side scattering signal (SSC), is related to the internal cellular complexity of the cells (Fig. 1a). Small subcellular structures, e.g., ribosomes, mitochondria, lipid bodies, or the cell nucleus, contribute to this signal[10, 11, 12, 13, 14, 15]. Despite this, most of the light will be scattered from the cells in forward direction (FSC), which reflects the size of the cells in some cell lines. Although most of the available knowledge of light scattering properties of cells is based on simulations

and experiments with animal or human cell lines, this reflects only partially the phenomena in plants and algal cells, respectively.

Based on the emission of fluorescent light, derived from intrinsic pigments of the photosynthetic apparatus, relative chlorophyll quantification in algal cells can be performed[16,17,18]. Thus, FC is an excellent tool in marine biology to identify and quantify different algal species. It has also been used to follow the DNA accumulation during cell cycle in synchronous *Chlamydomonas* cultures[19,20,21]. Lemaire and co-workers additionally used side scatter intensities to determine the sizes of isolated nuclei[19]. FC can be also used to study the arrest of DNA replication in cells due to the heat stress response[22]. The use of FC in algal biology has also been recently reviewed[23]. Quantitative interpretation of the signal measured by an FC device is usually based on an assumed linear dependency between the quantity of a cellular ingredient and the measured signal intensity. This holds true for numerous characterized parameters and cell lines but a potential deviation from linearity in FC devices may originate from an unfavorable relationship between laser beam geometry and cell size or shape (Fig. 1b)[24,25].

For decades, it has been known that synchronization of cell cultures increases the homogeneity of the cells compared to unsynchronized bulk cultures. Additionally, synchronization introduces a concerted developmental pattern that is highly reproducible and can be maintained for a virtually indefinite period in this synchronous state[26]. Due to their characteristics, synchronous cultures have been used in numerous studies as model cultures for study, e.g., cell cycle, photosynthesis, or metabolic events[2,27]. Light–dark synchronization is a known culturing method to synchronize photoautotrophic cells, such as algae, in a synthetic medium under a strict light–dark cycle that mimics the natural day–night cycle (e.g., 12 h light, 12 h dark)[28]. After each growth cycle, the cell suspension must be diluted with fresh medium to a fixed starting cell concentration[28] and after some days parallel development of cell growth, cell division, and daughter cell (DC) release is established[26,29,30].

Despite extensive use of FC in a number of different scientific disciplines and its huge potential, the technique has rarely been used to quantitatively study dynamics in synchronous algal cultures[31]. Many questions remain unanswered, such as how synchronicity is maintained over a virtually indefinite period, how exactly this is connected to the cellular metabolism, and what kind of physiological processes appear in parallel in all single cells, as would be expected from a naive perspective[31].

In this recent study, the potential of label-free FC for bioprocess monitoring was carried out, including a theoretical approach in which the importance of small intracellular components of algal cells with high refractive index (RI) and their contribution to the SSC was theoretically analyzed. The combination of the laser beam geometry in the FC device used and the described culture dynamics resulted in nonlinearity of the FC signals, which was much more pronounced than expected. Despite these obstacles, it was shown that the FC device can still be used for quantitative monitoring of culture dynamics. A major finding is a description of the still poorly known single-cell dynamics of synchronous cultures of *Chlamydomonas reinhardtii* on different levels that reveals that their complexity had been greatly underestimated. To the

best of our knowledge, the results reported in this paper constitute the first quantitative FC analysis of synchronized cultures of *Chlamydomonas reinhardtii*, which also includes quantitative considerations of how subcellular structures are involved in the light scattering process.

Results

Growth of cells in the model culture and technical limits of FC in relation to culture dynamics

During culture, a continuous light–dark regime (12 h (light) – 12 h (dark)) was applied to mimic a natural day–night cycle under controlled conditions. The light–dark cycles, followed by strict dilution with fresh culture media at the end of each dark period, resulted in a synchronization process (Figure 1c, d). The synchronization process is indicated firstly by an increase in mean cellular diameter during the light period. Secondly, the release of DC is initiated at the end of the light period and essentially completed after 6 h darkness (Figure 1c), and thirdly, the mean chlorophyll content per cell and the mean cellular diameter at the beginning and the end of the light–dark cycle is equal (Figure 1c, d), thus pointing to a repetitive culture development from one day to the next. The strain exhibited an approximately 12.6-fold increase in the cell number per suspension volume (Figure 1c).

The total chlorophyll content based on cell number, which was determined after solvent extraction, increased around 12.5-fold during the light phase (Figure 1d). During release of DC, the cell number-based chlorophyll content dropped rapidly. The results from the FC device clearly deviated from the extracted chlorophyll content, which was used as the reference method (Figure 1d). This can be explained by the relationship between culture development and laser beam geometry. Briefly, in an FC device, single cells pass through a laser beam, which creates a time-dependent signal (pulse) that can be analyzed in terms of its height, width, or area[24]. Usually, the pulse area is accepted as a suitable parameter for quantification of cellular fluorescence. For the flow cytometer used in this work, the pulse area greatly underestimated the chlorophyll quantity in the cells with a low chlorophyll quantity. This resulted in extreme widened chlorophyll distributions spread over more than three orders of magnitude toward zero (data not shown). The reason for this was an error in the software package from the FC manufacturer (personal communication from the manufacturer).

As an alternative to the pulse area, pulse height is a signal frequently used in FC. It has been described that the pulse height has a linear relationship with the emitted fluorescence of the cell if the diameter of the cell is less than the diameter of the laser beam, which is illustrated in Figure 1b[24,25]. The laser beam of the FC device used was elliptically shaped with a height of 60 µm and a width of 15 µm[25]. The latter dimension is the critical diameter through which the cells must pass[25]. In the case of model cultures of *Chlamydomonas* that were used, the cell culture dynamics exhibited conditions that potentially hinder data interpretation based on pulse height. Young DC at the beginning of the light phase are relatively small and exhibit a several fold increase in their cellular diameter. The mean diameter in the size distributions increased from 5.5 µm to 13 µm (Figure 1c) but did not exceed the critical diameter or width of the laser of 15 µm. Exemplary cell size distributions measured with a Coulter Counter device are shown

in Figure S1. A relatively small fraction of cells exceeded the laser beam diameter of 15 µm after 9 h of illumination. Thus, it can be expected that the chlorophyll quantity per cell will be underestimated for a relatively small proportion of cells. Experimental evidence of this underestimation is given in Figure 1c. A relative scale was used for the distinct time courses putting the first value at 1. Whereas the reference analysis displays an increase of around 12.5-fold in the chlorophyll content per cell, FC systematically underestimates the culture dynamics over time with an increase of only around 5-fold (Figure 1d). This difference was much greater than expected and was already present at 3 h of light. During this early stage of the light phase, only small algal cells can be observed.

Contribution of different cellular structures to the SSC

Based on the theoretical considerations of the Lorenz-Mie theory of light scattering, Figure 2 shows that the scattering intensity of lipid bodies and starch granules contributes much more to the SSC intensity (90° or 270°) than other cellular structures such as mitochondria or ribosomes. At a constant diameter of distinct particles, the high RI causes the pronounced contribution of lipid droplets and starch granules to the SSC. Briefly, 0° correspond to scattering in the original direction (FSC), 180° implies back-scattering, and 90° and 270° correspond to the side scatter signal (SSC). Data was were calculated using the tool MiePlot[32]. Details of the parameters used for Mie calculations and the corresponding scattered intensities at 90° are shown in Table 1. Despite the specific SSC contribution, most of the light that is scattered by lipid bodies, starch granules, and mitochondria (assumed diameter of 1 µm) is directed in the FSC direction (0°) (Figure 2a). Because of the small size of only 25 nm, angular scattering intensity of a single ribosome exhibits a much more isotropic scattering pattern and generally a very low scattering intensity (Figure 2b). The contribution of mitochondria to the SSC signal is comparatively low and the contribution of ribosomes is negligible (see also Table 1). Figure S4 shows the dependency of the scattering intensity on spherical starch granules of different sizes. Exemplary diameters of 0.5 µm, 0.75 µm, and 1.0 µm diameter were chosen. Despite the general change in the ratio between SSC (90°) and FSC (0°), the larger starch granules contribute more to the SSC intensity (90°), which means that the accumulation of starch during growth of the cells will contribute dynamically to the SSC signal.

Table 1

Simulation parameters used and calculated scattering intensity at 90°

Organelle	Diameter	Reference	RI	Reference	Parameters used in this study	Calculated scattering intensity at 90° (SSC)
Cytoplasm (reference)	-	-	1.36–1.375	Drezek et al. 1999[14]	RI = 1.36	-
Mitochondria	0.4–1 µm	Dunn A. & Richards-Kortum, 1996 [13]	1.38–1.41	Drezek et al. 1999[14]	RI = 1.41 d = 1 µm	0.061
Ribosome	25 nm	Manuell et al. 2005 [33]	1,39 - 1,42	Wang, 2000 [35]	RI =1.42 d = 25 nm	1.21×10^{-8}
Lipid body	0.20–2 µm	Wang et al. 2009 [34]	1.46	Jung et al. 2018 [36]	RI = 1.46 d = 1 µm	0.233
Starch granule	0–1.5 µm	Garz et al. 2012 [29]	1.50–1.54	Aas, 1996 [37]	RI = 1.5 d = 1.0 µm	0.397
Starch granule	0–1.5 µm	Garz et al. 2012 [29]	1.50–1.54	Aas, 1996 [37]	RI = 1.5 d = 0.75 µm	0.234
Starch granule	0–1.5 µm	Garz et al. 2012 [29]	1.50–1.54	Aas, 1996 [37]	RI = 1.5 d = 0.5 µm	0.102

Biologically relevant single-cell phenomena in synchronized model cultures

The cells exhibit large cell-to-cell heterogeneity in terms of chlorophyll quantity and SSC. Supplemental Figures S2 and S3 show the RCCC and SSC distributions at different times during the light phase of the diurnal cycle. The distributions are wide and show a spread of around one order of magnitude. The quantitative relation between SSC and the RCCC on the single-cell level is described below. Despite the nonlinearity described within the data sets for the larger cells, still valuable quantitative information about the cellular dynamics is included in the FC data. Briefly, within the optical setup of the FC device, emitted light (e.g., from chlorophyll) and the SSC intensity are gathered in the same optical path (in 90° direction) and are then separated into different spectral channels through optical components. Thus, the strengths of the nonlinearity of both signals can be estimated as identical and the relationship between both measures can still be used for label-free process monitoring.

Two-dimensional visualizations of the relationship between SSC and RCCC for the strain CC1690 are shown in Figure 3. At each single time point of the cellular development, the cell suspension has high cell-to-cell heterogeneity spreading across almost one order of magnitude. The cells exhibit a remarkable differentiation of the cell population into two subpopulations over time. Both subpopulations possess

highly different properties for RCCC and SSC (Figure 3, e.g., 11 h Light, 12 h Light). Based on the scatter cloud data, the SPEARMAN's rank correlation coefficient (SPEARMAN rho; test for general correlation) between the RCCC and SSC was calculated (Figure 4b). During most of the light phase the correlation coefficient ranges between 0.4 and 0.65 and shows a characteristic local maximum at 4 h light, which can be interpreted as a moderate correlation between RCCC and SSC. During the start of DC release at the end of the light phase, the correlation rises strongly to 0.85, which indicates a global correlation between the parallel appearance of mother cells and DC within the dataset. The time-dependent changes in the SPEARMAN rho (before the release of DC) indicate changes in the population structure and nonparallel development of the cells over time. In contrast to the low correlation at the single-cell level, calculated mean values for both parameter distributions are well correlated at all time points of the developmental cycle (Figure 4a). PEARSON rho (test for linear correlation) throughout all time points is 0.9923.

Discussion

SCA can describe cell-to-cell heterogeneities in cell populations that are not accessible with bulk methods. Some of the applications of SCA include medical diagnostics, basic research, and even bioprocess development in which heterogeneity within cell populations seems to play a major role. Understanding population dynamics might also be the key for greater productivity and product quality in large-scale production in biotechnology[3, 6, 38,39]. FC is probably the most commonly used single-cell analytical technology, because numerous commercial and user-friendly devices are available on the market. In the present study, the population dynamics in synchronous algal cultures, which have not been well characterized, were investigated as model processes in more detail by FC to reveal the potential of FC for label-free bioprocess monitoring. In addition to the experimental data, a theoretical approach was included to aid in interpretating the SSC signal in relation to cellular ingredients or structural parts of the cell.

Bulk dynamics in synchronized photoautotrophic cultures as a model process

FC was applied to a light–dark synchronized strain (CC1690) of *Chlamydomonas reinhardtii*. Photoautotrophic eukaryotic cells can often be synchronized by systematic application of light–dark periods and dilutions to equal cell density at the end of the dark phase (Banfalvi 2011)[40]. Under the described experimental conditions, the cells showed a characteristic change in cell number, mean cellular diameter, and chlorophyll accumulation over time. These general developmental stages are typical for light–dark synchronized algal cultures[29,30,41].

Validity of the chlorophyll fluorescence signal measured by FC and interpretation of the SSC signal in algal cells

In the past, it was shown that quantification of the chlorophyll amount per cell is technically feasible by using the intensity of the emitted chlorophyll fluorescence per cell as a quantitative measure[16,17,18,42]. The linearity of the FC data is not always guaranteed. The most likely explanation is an unfavorable

combination of cell size and geometry of the laser beam within the FC device used when using pulse height to measure the fluorescence intensity[24,25]. This leads to an underestimation of the FC signal. For polydisperse cell size distributions, this ultimately will lead to an underestimation of cell-to-cell heterogeneity by the FC device. Under the specific conditions used in this study, systematic underestimation of the detected chlorophyll fluorescence intensity by the FC device was described in relation to the reference analysis (Figure 1). The underestimation was much higher than expected and already affected relatively small algal cells after 3 h of illumination. Nevertheless, the mean of the cell size distribution as determined by Coulter Counter measurements never exceeded the laser beam diameter of 15 µm (Figure 1). Even during the latest time points within the light phase, only a small proportion of cells exceeded the laser diameter (Figure S2). In addition to the cell size changing over time, another specific property of *Chlamydomonas* cultures might cause the unexpected deviation from reference techniques. During most of the developmental cycle, cells of *Chlamydomonas* have a typical elliptical shape[31], but regardless of the "real" cell shape, the Coulter Counter device displays the determined cell sizes as the equivalent sphere diameter, assuming a spherical shape of the particles after quantifying the particle volume[42]. In addition to this, the movement of the cells through the flow cuvette is supported in FC devices with a laminar flow pattern within the carrier liquid enabling hydrodynamic fixation of the cells. Thus, elliptical cells will be aligned with their longer diameter parallel to the flow direction while moving through the flow cuvette. This virtually increases the diameter of the cells during their interaction with the laser beam. This very likely leads to the pronounced underestimation of the chlorophyll content that was observed even with relatively small cells in synchronized cell cultures of *Chlamydomonas*.

The measured SSC intensity derived from a single cell is based on the interplay between different parameters[11,12,13,14,15]. Briefly, a single cell can be understood as a particle with different constituents in different volume fractions. The different constituents can be approximated as granular structures with given RI and different diameters. It is well accepted that the SSC signal depends on the cellular complexity of the single cells in which different small subcellular granular structures, such as mitochondria, contribute strongly to the SSC intensity[11,12,13,14,15]. To the best of our knowledge, this interpretation has so far been restricted to non-photosynthetic cells. Recent calculations based on the Lorenz-Mie theory of light scattering revealed that most likely lipid bodies and starch granules contribute to this signal within algal cells, with the starch granules having the highest SSC intensity (Figure 2, Table 1, Figure S4). Calculations were made with the freeware tool MiePlot, which was originally created for quantitative analysis of scattering phenomena in the atmosphere[32]. The large difference between the reference RI (approximated as RI from cytoplasm) and RI of starch granules and lipid droplets causes the high contribution of both storage compounds to the SSC signal in algal cells. This contribution is greater than that of mitochondria and much greater than the contribution of a ribosome.

The described nonlinearity in the chlorophyll fluorescence signal will also be present in other commercially available FC devices that share a similar laser beam geometry[25], making it of great interest for the scientific community or in industrial applications. Questions arise about how the nonlinearity may

affect the SSC signal and how the performance of the FC device is disrupted for quantitative cell characterization. The nonlinearity and thus the underestimation of cell-to-cell heterogeneity will also be present in the SSC signal, because emitted light and the SSC intensity are gathered in the same optical path (in 90° direction) and are subsequently separated into different spectral channels through optical components. Thus, the underestimation should be identical for SSC and chlorophyll fluorescence within each distinct cell. The data generated by the FC device is still of high value for bioprocess monitoring and can be applied in various situations. First, cell-to-cell heterogeneity is underestimated for larger and elliptical cells but it can still be determined and used for semi-quantitative culture characterization or quality controls in biotechnological production processes. Second, subpopulations can still be visualized and identified under the described circumstances. Third, as SSC and chlorophyll fluorescence are gathered within the same optical path of the device, the specific relationship between both parameters can still be used as a quantitative measure for bioprocess monitoring. Such possible sensitive measures include determination of covariance and correlation coefficients over the processing time. These considerations have been further applied on the fast-growing model culture.

Single cell dynamics determined by FC measurements

For decades, it has been known that synchronization of cell cultures increases homogeneity of the cells compared to unsynchronized bulk cultures. Results from this study show that synchronized *Chlamydomonas* cells possess unexpected cell-to-cell diversity both in chlorophyll content (RCCC) and SSC (Figure S2 and S3, Figure 3). The observed heterogeneity was not diminished after “re-cloning” the cells before preparation of the pre-culture. This means that the cell-to-cell heterogeneity was not based on genetic diversity in the cell culture. A high correlation between RCCC and SSC was found throughout the developmental cycle of the cells, regarding the means of the distributions (Figure 4). This matches the interpretation of both parameters for photosynthetic cells, which covers the cellular complexity, including storage compounds (starch and lipid droplets) in particular, within the parameter SSC, and the chlorophyll quantity (RCCC), which relates to the size of the photosynthetic apparatus within each cell. From a naive perspective, a cell containing a large amount of chlorophyll might also exhibit a high photosynthetic capability and thus should be able to accumulate a large quantity of storage compounds, coded by the SSC. Surprisingly, a relatively low correlation between both parameters was described at the single-cell level at each distinct time point (Figure 3 and Figure 4). Over time, the correlation changed, which implies nonparallel development of the cells. A very detailed analysis of starch-related single-cell dynamics in synchronous algal cultures was carried out by Garz and co-workers using an advanced microscopic imaging approach, based on Second Harmonic Generation microscopy[29]. They described a low and dynamic correlation between single-cell starch content and cellular volume in synchronized *Chlamydomonas* cells. Additionally, the former study also analyzed single-cell starch degradation rates during the night phase, indicating a complex mode of starch degradation that requires largely unknown regulatory mechanisms. The cells in the present study have been grown under identical conditions but the focus was more on development of the cells during the light phase. A high cell-to-cell heterogeneity for the starch content has been also shown in microscopic images with other strains of *Chlamydomonas*[30].

Additionally, the recent study described a remarkable differentiation of the cell population into two subpopulations during the time of culture. Both subpopulations possess highly different properties in terms of RCCC and SSC, but the exact biological implications remain unclear (Figure 3, e.g., 10 h light, 11 h light).

Finally, the question arises about what drives the deviating developmental paths and the high cell-to-cell heterogeneity. In the past, many studies tried to identify the reason for heterogeneity in different cell cultures. For example, detailed analyses of bacterial cells clearly revealed that isogenic DC exhibit significant heterogeneity for copy numbers of many proteins and transcripts[43,44]. It is believed that stochasticity of gene transcription or within other highly regulated cellular events is the key driver[43]. One of these highly regulated cellular events might be the physiological response of synchronized algal cells to the applied light–dark cycle, altering the photosynthetic apparatus. Pigment composition measurements and functional analysis of the photosynthetic apparatus of two synchronized strains of *Chlamydomonas* (CC125 and CC3491) implied non-equal accumulation over time of major multiprotein complexes of the photosynthetic apparatus, such as light harvesting and core complexes[30]. More detailed analysis of molecular events in synchronous cultures was carried out using two very advanced systems biology approaches that indicated complex physiological responses by the synchronized *Chlamydomonas* strains to the diurnal rhythm[2,27]. It was shown, for example, that around 85% of the genes were differentially expressed during different phases of the light–dark cycle, which illustrates concerted alteration within the cellular physiology[2]. The three studies illustrate numerous physiological alterations of *Chlamydomonas* due to the light–dark cycle that are ultimately linked at the molecular level to highly stochastic events[43]. Additionally, asymmetric partitioning of storage compounds and asymmetric cell division were considered in a theoretical approach as the reason for cell-to-cell heterogeneity, and it was concluded that a complex combination of different phenomena is necessary to explain the heterogeneity in synchronous cultures[41]. It appears that the cell-to-cell heterogeneity inside synchronized *Chlamydomonas* cultures is intrinsically driven and seems to be rather common and not an unusual trait.

Combined with these internal factors, external factors affecting the cell population might also be important. For algal cells, homogenous illumination and supply of nutrients including CO_2 inside the culture vessel might be of great importance. To understand the external factors in more detail, a systematic analysis of mixing times, mass transfer, and light distribution should be performed in future for the photobioreactors used (devices used to culture the photoautotrophic cells).

The current study has shown that FC can be used for label-free process monitoring. The knowledge gained about the strong contribution of starch granules and lipid bodies inside the algal cells to the SSC signal in particular opens new paths for bioprocess monitoring in algal cultures, an as yet unexplored topic, especially in industrial production processes. Recent studies have shown the potential of analysis of distinct light-scattering properties of cell cultures using a novel technique called Photon Density Wave spectroscopy as a valuable tool for bioprocess monitoring[45,46].

Another clear improvement to classical FC is the use of on-line FC in which the FC device is capable of automated sample analysis with very high time resolution[7,47]. Independently of the extensive usage of FC in different scientific disciplines and its huge potential, single-cell analysis has rarely been used to quantitatively study dynamics in synchronous algal cultures[31].

Conclusion

This study revealed that (i) storage compounds (lipid bodies and starch granules) within algal cells are very likely the most important contributors to the commonly used wide-angle light scattering signal in flow cytometry devices, (ii) specific cellular growth dynamics of the synchronous algal cultures induced a pronounced nonlinearity in the cytometry data which resulted in distorted chlorophyll and wide-angle scatter distributions, (iii) apart from the nonlinearity described, the technique is still applicable as a sensitive label-free tool for bioprocess monitoring, (iv) high cell-to-cell heterogeneity within cellular chlorophyll amount and the wide-angle light scattering signal was described in synchronous algal cultures, (v) cellular chlorophyll amount and the wide-angle light scattering signals shared a relatively low but dynamic correlation over time, and (vi) the synchronous algal cultures exhibited nonparallel development of the algal cells.

Materials And Methods

Biological materials

Chlamydomonas reinhardtii strain CC1690 wild type mt^+ [Sager 21gr] was obtained from the *Chlamydomonas* Resource Center, University of Minnesota, USA.

Preculture and synchronization

Chlamydomonas cells were precultured for five days at room temperature in a medium containing five macrocompounds according to [48] and trace elements modified according to[28]. Subsequently, cells were synchronized in the same medium (34°C; 12 h light/12 h dark; continuous agitation by air enriched with 2% [v/v] CO_2, dilution to 7×10^5 cells ml^{-1} before each light period). Both preculture and synchronization were performed under axenic conditions. For details, see[29,30]. The whole procedure was performed with two independent biological replicates.

Quantification of cell number and cell size

Cell number and cell size were determined using a Beckman Coulter Counter ‘MULTISIZER 3’ (Beckman Coulter, Krefeld, Germany). Measurements are based on at least 2×10^4 cells.

Flow cytometry

FC was performed using a CyFlow Space instrument (Partec, Münster, Germany). A laser with a wavelength of 488 nm was used to determine the relative cellular chlorophyll content (RCCC) and side scatter signal (SSC). After excitation with the laser, emitted chlorophyll fluorescence was passed through a band pass filter (central wavelength 675 nm). Fifty thousand cells were analyzed for each sample. Count rates did not exceed 1,000 counts per second. Data were collected with Partec FloMax software version 2.5 (Partec, Münster, Germany) and further analyzed by a program written in MATLAB® version 2016 (The MathWorks, Nattick, USA).

Chlorophyll extraction

Cells (2 ml suspension each) were collected by centrifugation (5 min at 5,000 ´ *g*), frozen in liquid nitrogen, and then stored at -80°C until use. Following resuspension in 1 ml 80% [v/v] acetone, cells were incubated for 10 minutes at room temperature and then ruptured by ultrasonification (4 ´ 8 s each; 25% maximum power; Sonopuls, Bandelin Electronic, Berlin, Germany). Homogenates were centrifuged at 10,000 ´ *g* for 5 min. The supernatants were used for further analysis.

Chlorophyll quantification

Total chlorophyll content in the supernatant was determined photometrically[49].

Simulated side scatter intensities of various cell ingredients

Side scatter intensities were calculated based on Lorenz-Mie theory of light scattering with the freeware tool MiePlot version 4.6.21[32,50]. The tool plots functions for scattering amplitude as a function of wavelength, particle size, and material properties. Most important parameters that must be fixed are diameter of the spherical particle, RI of the sphere, RI of the surrounding medium, and the wavelength of the incident light. Unpolarized incident light with a wavelength of 488 nm was used for calculations. Details of the chosen parameters and reference data from different sources are given in Table 1.

Statistical analysis

Statistical analyses (arithmetic mean, standard deviations, and correlation analysis) were performed with SigmaPlot® version 14 (Systat Software GmbH, Düsseldorf, Germany).

Declarations

Data Availability.

The datasets generated during and/or analyzed during the current study are available from the corresponding author on reasonable request.

Author contribution.

MS and MR conducted the experiments, collected data, and analyzed the datasets. MS programmed the algorithm written in MATLAB for analysis of the FC data and performed the calculations according to the Lorenz-Mie light scattering theory. MS and MR prepared the manuscript. All authors read and approved the final manuscript.

Acknowledgments.

We thank Dr. Lena Bressel and Dr. Oliver Reich for the discussions about light scattering and interaction of spherical particles with a laser beam. We further gratefully acknowledge Prof. Dr. Martin Steup for the in-depth discussions about cell-to-to cell heterogeneity in cell cultures.

Competing interests.

The authors declare no competing interests.

References

1. Ghatak, A., Chaturvedi, P. & Weckwerth, W. Cereal Crop Proteomics: Systemic Analysis of Crop Drought Stress Responses Towards Marker-Assisted Selection Breeding. *Front. Plant Sci.***8**, 757 (2017).
2. Strenkert, D. *et al.* Multiomics resolution of molecular events during a day in the life of Chlamydomonas. *Proc. Natl Acad. Sci. USA* **116**, 2374–2383 (2019).
3. Fritzsch, F. S. O., Dusny, C., Frick & Schmid, O. A. Single-Cell Analysis in Biotechnology, Systems Biology, and Biocatalysis. *Annu Rev Chem Biomol Eng***3**, 129–155 (2012).
4. Delvigne F., Zune, Q., Lara, A. R., Al-Soud, W. & Sørensen, S. J. Metabolic variability in bioprocessing: implications of microbial phenotypic heterogeneity, *Trends Biotechnol*.**32**, 608–616 (2014).
5. Rosenthal, K., Oehling, V., Dusny, C. & Schmid, A. Beyond the bulk: disclosing the life of single microbial cells. *FEMS Microbiol Rev.* **41**, 751–780 (2017).
6. Sandmann, M., Lippold M., Schafberg M. & Rohn S., Analysis of population structures of the microalga Acutodesmus obliquus during lipid production using multi-dimensional single-cell analysis, *Sci. Rep.*, **8**, 6242 (2018).
7. Delvigne, F. *et al.* Taking control over microbial populations: Current approaches for exploiting biological noise in bioprocesses. *Biotechnol. J.,***12**, 1600549 (2017).
8. Picot, J., Guerin, C. L., Le Van Kim, C. & Boulanger, C. M. Flow cytometry: retrospective, fundamentals and recent instrumentation. Cytotechnology. **64**,109–30 (2012).
9. Dubelaar, G. B. J. & Jonker, R. R. Flow cytometry as a tool for the study of phytoplankton. *Sci Mar*. **64**, 135–56. (2000).
10. Shapiro, H. M. Microbial analysis at the single-cell level: tasks and techniques. *J Microbiol Methods*. **42**, 3–16. (2000).

11. Bohren C. F. & Huffman, D. R. Absorption and Scattering of Light by Small Particles. (WILEY-VCH, 2004).
12. Mourant, J. R. et al. Mechanisms of light scattering from biological cells relevant to noninvasive optical-tissue diagnostics. *Appl. Opt.***37**, 3586–3593 (1998).
13. Dunn A. & Richards-Kortum R. Three-Dimensional Computation of Light Scattering From Cells. *IEEE J Sel Top Quantum Electron*, **2**, 898–905 (1996).
14. Drezek, R., Dunn, A. & Richards-Kortum, R. Light scattering from cells: finite-difference time-domain simulations and goniometric measurements. *Appl. Opt.***38,** 3651–3661 (1999).
15. Ulicny, J. Lorenz-Mie light scattering in cellular biology. *Gen. Physiol Biophys*. **11**, 133–151 (1992).
16. Hashemi, N., Erickson, J. S., Golden, J. P. & Ligler, F. S. Optofluidic characterization of marine algae using a microflow cytometer. *Biomicrofluidics*. **3**,32009–320099 (2011).
17. Jacquet, S., Lennon, J-F., Marie, D. & Vaulot, D. Picoplankton population dynamics in coastal waters of the northwestern Mediterranean Sea. *Limnol Oceanogr*. **43**, 1916–31 (1998).
18. Vaulot, D. & Marie, D. Diel variability of photosynthetic picoplankton in the equatorial Pacific. *J Geophys Res Atmos*. **104**, 3297–310 (1999).
19. Lemaire, S. *et al.* Analysis of light/dark synchronization of cell-wall-less *Chlamydomonas reinhardtii* (Chlorophyta) cells by flow cytometry. *Eur. J. Phycol.***34**, 279–286 (1999).
20. Mahjoub, M. R. *et al*. The FA2 gene of Chlamydomonas encodes a NIMA family kinase with roles in cell cycle progression and microtubule severing during deflagellation. *J Cell Sci.***115**, 1759–68 (2002).
21. Fang, S. C., de los Reyes, C., Umen, J. G. Cell size checkpoint control by the retinoblastoma tumor suppressor pathway. *PLoS Genet*. **2**, e167 (2006).
22. Hemme, D. *et al.* Systems-wide analysis of acclimation responses to long-term heat stress and recovery in the photosynthetic model organism Chlamydomonas reinhardtii. *Plant Cell.***26**, 4270–97 (2014).
23. Hyka, P., Lickova, S., Přibyl, P., Melzoch, K. & Kovar, K. Flow cytometry for the development of biotechnological processes with microalgae. *Biotechnol. Adv.* **31**, 2–16 (2013).
24. Shapiro H. M. How Flow Cytometers Work in *Practical Flow Cytometry*. 101–223 (Wiley-Liss., 2003).
25. Rothe, G. Technical Background and Methodological Principles of Flow Cytometry in *Cellular diagnostics: basic principles, methods and clinical applications of flow cytometry*. (ed. Sack, U., Tárnok, A., & Rothe, G.) 53–88 (Karger Medical and Scientific Publishers, 2009).
26. Vítová, M. et al. Chlamydomonas reinhardtii: duration of its cell cycle and phases at growth rates affected by temperature. Planta 234, 599–608 (2011).
27. Zones, J. M., Blaby, I. K., Merchant, S. S. & Umen, J. G. High-Resolution Profiling of a Synchronized Diurnal Transcriptome from Chlamydomonas reinhardtii Reveals Continuous Cell and Metabolic Differentiation. Plant Cell. 27, 2743–2769 (2015).

28. Kuhl, A. & Lorenzen, H. Handling and culturing of chlorella in Methods in cell physiology. (ed. Prescott D. M.) 159–187. (Academic Press, 1964).
29. Garz, A., et al. Cell-to-cell diversity in a synchronized Chlamydomonas culture as revealed by single-cell analysis. *Biophys. J.* **103**, 1078-1086 (2012).
30. Sandmann, M., Garz, A. & Menzel, R. Physiological response of two different Chlamydomonas reinhardtii strains to light-dark rhythms. Bot. 94; 153–64 (2016).
31. Umen, J. G. Sizing up the cell cycle: systems and quantitative approaches in Chlamydomonas, *Curr. Opin. Plant Biol.***46**, 96–103, 2018.
32. Laven P. A Computer Program for Scattering of Light From a Sphere Using Mie Theory & the Debye Series http://www.philiplaven.com/mieplot.htm (2021).
33. Manuell, A. L., Yamaguchi, K., Haynes, P. A., Milligan, R. A. & Mayfield, S. P. Composition and structure of the 80S ribosome from the green alga Chlamydomonas reinhardtii: 80S ribosomes are conserved in plants and animals. *J Mol Biol*. **351**, 266–279 (2005).
34. Wang, Z. T., Ullrich, N., Joo, S., Waffenschmidt, S. & Goodenough, U. Algal lipid bodies: stress induction, purification, and biochemical characterization in wild-type and starchless Chlamydomonas reinhardtii. *Eukaryot Cell*. **8**, 1856–1868 (2009).
35. Wang, R. K. Modelling optical properties of soft tissue by fractal distribution of scatterers. *J. Mod. Opt.* **47**, 103–120 (2000).
36. Jung, J. *et al.* Label-free non-invasive quantitative measurement of lipid contents in individual microalgal cells using refractive index tomography. *Sci Rep***8**, 6524 (2018).
37. Aas, E. Refractive index of phytoplankton derived from its metabolite composition, *J. Plankton Res.***18**, 2223–2249 (1996).
38. Glassey, J. et al. Process analytical technology (PAT) for biopharmaceuticals. *Biotechnol. J.***6**, 369–377 (2011).
39. Lencastre F. R. et al. Experimental methods and modeling techniques for description of cell population heterogeneity. *Biotechnol. Adv.***29**, 575–599 (2011).
40. Banfalvi, G. Overview of cell synchronization. *Methods Mol Biol*. **761**, 1–23 (2011).
41. Rading, M. M., Sandmann, M., Steup, M., Chiarugi, D. & Valleriani, A. Weak correlation of starch and volume in synchronized photosynthetic cells. Phys Rev E Stat Nonlin Soft Matter Phys. **91**, 012711 (2015).
42. Sandmann, M., Lippold, M., Saalfrank, F., Odika, C. P. & Rohn, S. Multi-dimensional single-cell analysis based on fluorescence microscopy and automated image analysis, Anal. Bioanal. Chem. **409**, 4009–4019 (2017).
43. Lloyd-Price, J. *et al.* Probabilistic RNA partitioning generates transient increases in the normalized variance of RNA numbers in synchronized populations of Escherichia coli. *Mol. Biosyst*. **8**, 565–571 (2012).

44. Taniguchi, Y. P. J. *et al*. Quantifying E. coli proteome and transcriptome with single-molecule sensitivity in single cells. *Science*. **329**, 533–538 (2010).
45. Gutschmann, B. et al. In-line monitoring of polyhydroxyalkanoate (PHA) production during high-cell-density plant oil cultivations using photon density wave spectroscopy. *Bioengineering*. **6**, 85 (2019).
46. Sandmann, M., Münzberg, M., Bressel, L., Reich, O. & Hass, R. Inline monitoring of high cell density cultivation of Scenedesmus rubescens in a mesh ultra-thin layer photobioreactor by photon density wave spectroscopy. *BMC Res. Notes*. **15**, 54 (2022).
47. Haberkorn, I., Off, C. L., Besmer, M. D., Buchmann, L. & Mathys, A. Automated Online Flow Cytometry Advances Microalgal Ecosystem Management as *in situ*, High-Temporal Resolution Monitoring Tool. *Front. Bioeng. Biotechnol.***9,** 642671 (2021).
48. Sueoka, N. Mitotic replication of deoxyibonucleic acid in Chlamydomonas reinhardtii. *Proc. Natl. Acad. Sci. USA.***46**, 83–91 (1960).
49. Lichtenthaler, H. K. & Buschmann, C. UNIT F4.3 Chlorophylls and carotenoids: measurement and characterization by UV–VIS i*n Current protocols in food analytical chemistry.* (Wiley Online Library 2001).
50. Mie, G. Beiträge zur Optik trüber Medien, speziell kolloidaler Metallösungen. Ann Phys. **330**, 377–445 (1908).

Figures

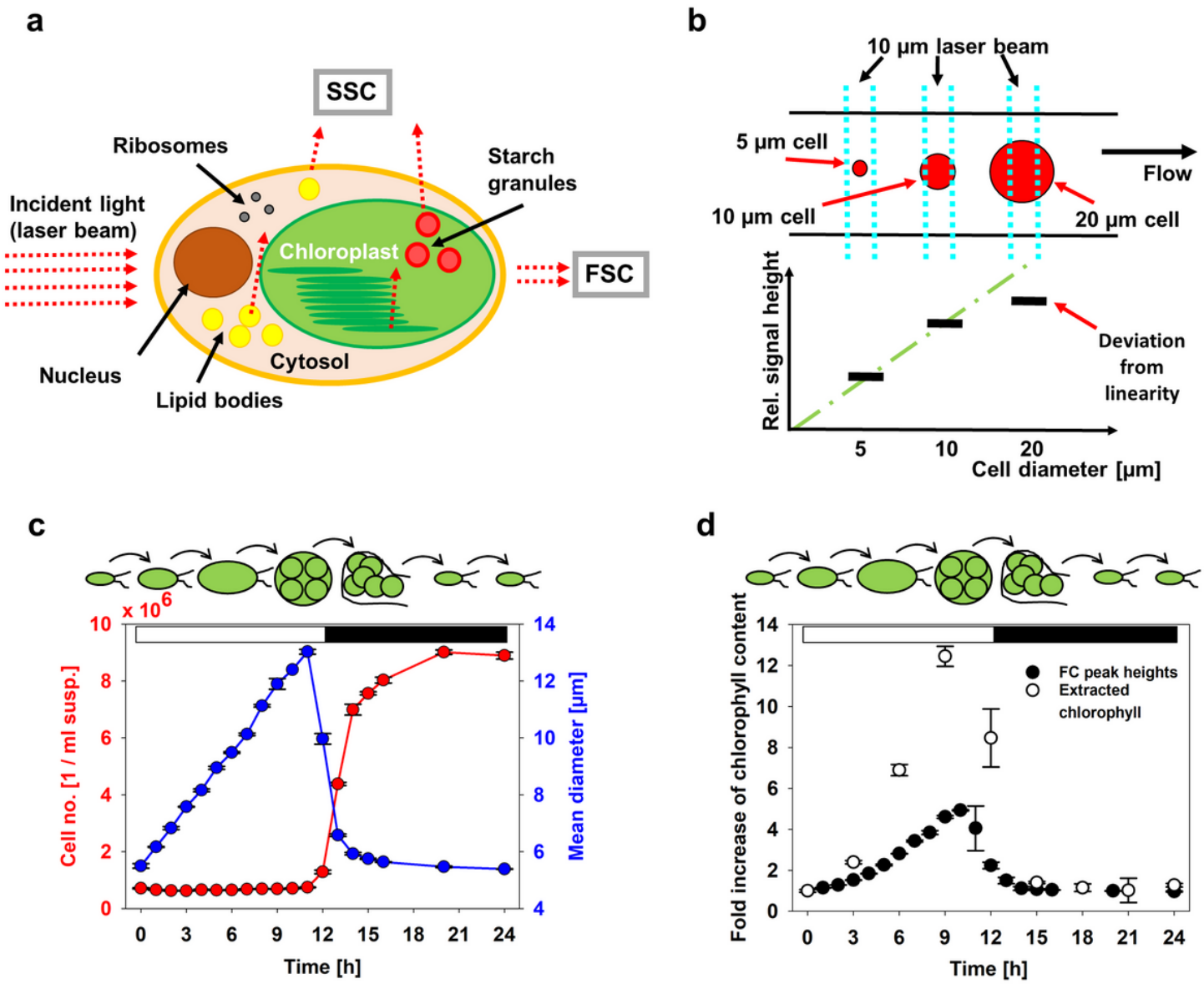

Figure 1

Relationship between cellular properties and results derived from flow cytometry. (a) Schematic drawing of the expected contribution of cellular structures to different light scattering angles. Subcellular structures, e.g., ribosomes, or lipid bodies contribute significantly to the side scatter signal (SSC). Scattered light in the forward direction (FSC) reflects cellular size. (b) Cells of different diameters passing through the laser beam. The largest cell has a larger diameter than the laser beam, which results in an underestimated signal height. (c) Cell number based on suspension volume and the mean cellular diameter are plotted against time of the light–dark cycle (12 h light, 12 h darkness). Mean ± SD are given (n = 4). (d) Development of total chlorophyll content obtained by solvent extraction (open circles) and flow cytometry (closed circles) are given as fold increase in relation to 0 h light. Mean ± SD are presented (extraction: n = 4; FC: n = 2). The open and filled bars indicate the light and dark phases, respectively. Schematic drawing of the developmental cycle of the cells in relation to the experimental data shown in green (c, d).

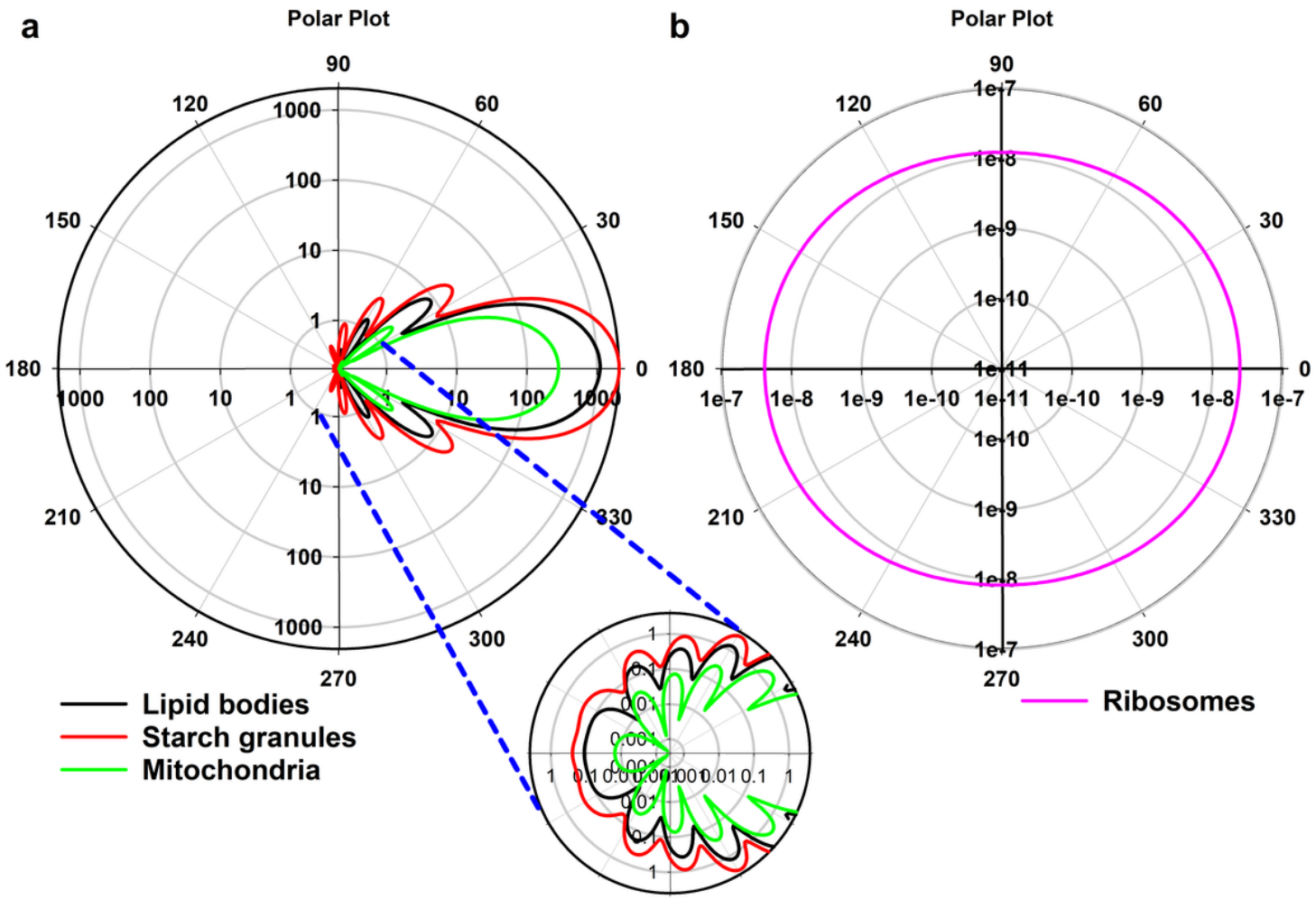

Figure 2

Scattering angle dependent intensity distributions calculated using Mie theory for different sub-cellular constituents. (a) Polar plot of scattered intensity vs. scattering angle for a lipid body, starch granule, and mitochondria, respectively. The insert shows an enlarged area. (b) Polar plot of scattered intensity vs. scattering angle from a ribosome. Intensity distributions have been calculated using the freeware tool MiePlot[32].

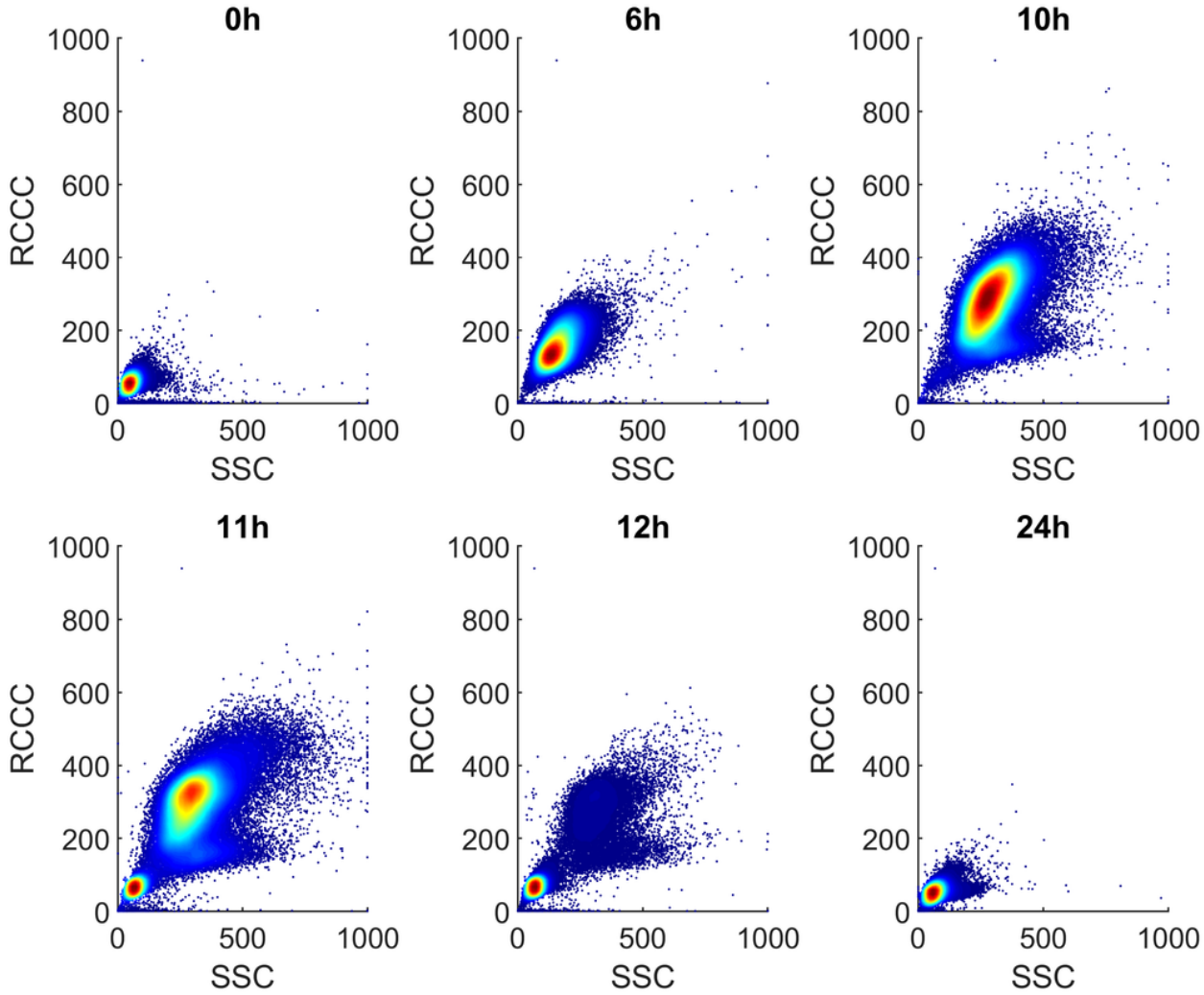

Figure 3

Scatter plots of SSC and relative cellular chlorophyll content (RCCC) determined by single cell analyses. Each dot represents one characterized cell. At each time point 50,000 cells were analyzed. Warm and cold colors represent high and low number of cells inside the particular diagram area, respectively.

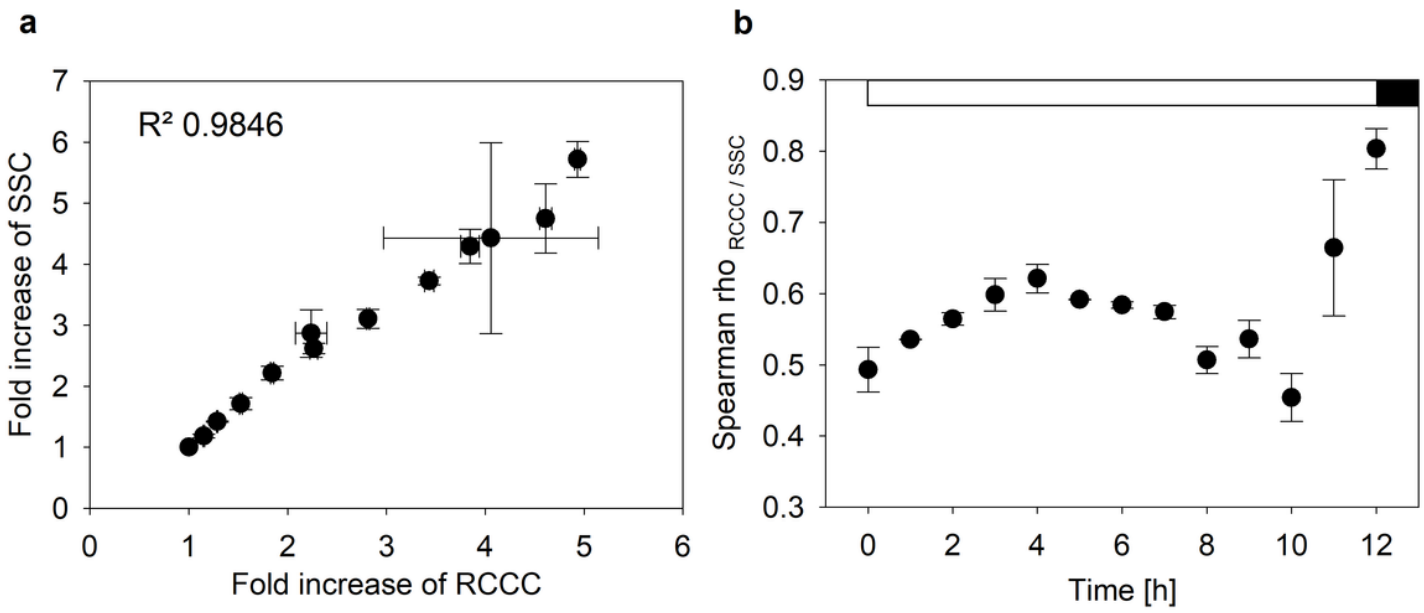

Figure 4

Relationship between relative cellular chlorophyll content (RCCC) and cellular SSC during algal growth. (a) Correlation between calculated mean values for SSC and RCCC shown as fold increase in relation to 0 h light. (b) Correlation between SSC and RCCC within the distinct two-dimensional distributions. Mean ± SD are given (n = 2).

Supplementary Files

This is a list of supplementary files associated with this preprint. Click to download.

- SupplementalMaterial.pdf